DOT GAIN ANALYSIS OF ROUND PRINTING ELEMENTS CREATED BY APPLYING METALIZED FOIL USING THE COLD-HOT FOIL LAMINATION PROCESS

IGOR MAJNARIĆ,* MORIĆ MARKO,** MATKO PINTAR*** and DAMIR MODRIĆ*

*University of Zagreb, Faculty of Graphic Arts, Getaldićeva 2, 10000 Zagreb, Croatia
**University of North, Department of Art Studies, Žarko Dolinar Square 1, Koprivnica, Croatia
***SATO d.o.o. Vodovodna ulica 2, 49 210 Zabok, Croatia
✉ Corresponding author: I. Majnarić, majnaric@grf.hr

The major objective of this paper consists in acquiring new knowledge and understanding the interaction between the printed metalized foil and the paper printing substrate. Since the Inkjet printing principle is often used for the adhesion of metalized foils (cold-hot process), it is necessary to investigate the influence of piezo Inkjet head settings on the final imprint. The light distribution on the halftoned metalized print depends on the optical properties of the paper and the metalized foil. Therefore, the problem of accurate reproduction is divided into the distribution of light in the paper and the reflection from the printed round metalized printing elements. For ImageJ software (gold dot imprint photographs), two physical quantities were analyzed (realized edge parts and anisotropic scattering of light from the printed surface = dot gain), which ultimately achieved a change in the realized dimension of print elements.

In this paper, the authors present a new method for testing the efficiency of halftones (50% TV surface coverage) created with four diameters of gold foil printing dots (0.100 mm; 0.250 mm; 0.500 mm; 0.750 mm) applied to matte fine art cardboard. The experiment involved a gradual variation of the amount of UV-cured Inkjet varnish used, which played a crucial role in the production of metallic visual dot samples. To assess the effectiveness of this method, three different thicknesses of UV-cured varnish (29 µm, 43 µm, and 58 µm) were used in conjunction with modular Konica Minolta Jetvarnish 3DS machine (piezo Inkjet heads KM1024 iLHE-30), and constant printing speeds of 0.30 m/s. The research findings indicate that a 29 µm layer thickness of UV varnish and the substrate moving in cross-direction are optimal for producing cold metalized foil lines. However, the results also show that a more significant application of varnish offers a better chance of reproducing the dot and achieving a better contrast. The results show that elements smaller than 0.250 mm cannot be realized and that the print optimum will be achieved with UV Inkjet varnish application settings greater than 29 µm and less than 43 µm.

Keywords: half-tone metalized surface, UV Inkjet varnish, fine art paper, cold-hot lamination, dot gain

INTRODUCTION

The need to reproduce multicolored images and text is as old as printing. At the beginning of printing, printing machines could not satisfy these requirements because, technologically, wooden printing forms prevailed, which were hand-engraved and could not reproduce relatively rough black or white linear surfaces. The improvement of the image reproduction technique, the use of engraved copper plates, and the use of lithography made it possible to reproduce microscopic printed elements. However, it was only with the discovery of the photographic process (some 150 years ago) that the potential development of continuous tone reproduction was realized. Georg Meisenbach laid the foundation for screened reproduction by introducing the autotype screening process into the graphics industry, which is still in use today with minor modifications. Rasterization converts the continuous tones of the original (photo) into one tone (black and white information of many small raster elements). A completely identical procedure is used in the realization of color-tone images. Applying process colors (cyan, magenta, and yellow) makes achieving an optimal gray

balance and reproduction of several different color tones possible.[1,2]

Digital printing machines apply a digital screening process and work on a similar principle. Digital printing systems, such as Inkjet, use a unique digital screening process, where droplets (smallest print elements) are released, forming halftones by the principle of generating frequency-modulated screening (diffusion error or dithering method). Thus, the printing substrate's spreading liquid will create a larger physical dot gain. At the same time, the absorbency of the paper printing substrate is crucial.[3]

In most printing processes, binary printing is used (ink on paper on one level with only two options for transferring ink to the substrate – imprint or not imprint). Shades of gray tones are achieved by printing small patterns of geometric elements (often dots) and varying the surface coverage with printing elements (F). It can be achieved by changing the size of the raster elements or by realizing a different concentration (grouping) with the size of the same screen elements. The visual uniformity of the print with the original is achieved by the additional effect of integration, which is carried out by the human eye during the observation process from a certain distance.[4]

In digital graphic reproduction, dot gains of screen values (transfer of print elements from a digital file to paper) are determined with a reflection densitometer. In doing so, the difference between the theoretically determined total area of screen elements (Tone value original) and the actualized area with screen tone elements printed on the paper (Tone value print) is determined. Due to the technical imperfection of the printing system and the effect of light capture, printing without increasing the print elements (dot gain) is impossible. Therefore, dot gain has long been recognized as one of the most critical factors associated with print quality. Numerous studies indicate that during average printing on gloss fine art paper with a new-generation printing machine, a dot gain of between 12% and 22% is shown at 50% TV (TV = tone value). The fact that average printing is mentioned indicates that the dot gain can be lower but higher than the stated values.[5]

Dot gain in the printing process

To successfully determine the optical dot gain with a densitometer, it is necessary to decide on the properties of the paper (the whiteness of the printing substrate) and the solid print (the layer of printed ink). This is not possible with a metalized print because of uncontrolled specular reflection. Printing a modified metalized surface on white paper does not achieve satisfactory dot gain results, and the standard process of monitoring print quality based on the determination of the tone value increase (using optical densitometry) cannot be used successfully. Therefore, in this paper, the authors try to approach the determination of dot gain with a new (own) method of image analysis based on printing gold surfaces with round raster elements. This approach is new and gives the possibility of analyzing the realized optical and physical dot gain on the metalizing surface.

The first approximate solution to the dot gain problem was given by Schuster (1905), who assumed that light radiation acts only forward and backward.[4] Kubelka and Munk (1931) developed their well-known model under this influence.[6,7,8] After the 1930s, the Kubelka-Munk theory underwent some changes and corrections. At the end of the 1940s, Saunderson introduced the reflection at the border of adjacent layers into the calculation, making the theory more applicable to real-world scenarios. At the same time, Kubelka later tried to improve the model by applying it to optically inhomogeneous media, in which the ratio of absorption and scattering is constant.[7,9] Emmel and Hersch introduce an elegant matrix-based mathematical formulation of the Kubelka-Munk theory that allows them to apply this theory to images printed by raster reproduction, demonstrating its practicality.[10,11] The Mourad dissertation extended the one-dimensional representation of the Kubelka-Munk theory (2 streams) to three dimensions (6 streams), which enabled the inclusion of light scattering in the paper substrate and, thus, an accurate description of the optical dot gain, further highlighting its relevance.[12]

Physical dot gain

Physical dot gain, also known as mechanical dot gain, refers to the physical increase in the size of printed dots compared to their intended digital size. This phenomenon is caused by the spreading of printing ink beyond the edges of the original dot during the printing process, mainly due to factors such as ink absorption into the substrate and the mechanical properties of the printing system. As a result, the printed dot appears more significant than the theoretical digital dot, increasing tone value and potential distortion in

image quality. The primary cause of mechanical dot gain is the scattering and absorption of ink at the edges of the printed dot. When ink is applied to paper, it spreads laterally due to the paper's absorbency and the properties of the ink. The choice of paper is crucial: coated papers are designed to resist ink absorption, leading to less mechanical dot gain, while uncoated papers allow the ink to absorb more freely, resulting in a more pronounced increase in dot size. Therefore, careful selection of paper is essential in managing mechanical dot gain.[13]

On coated papers, the ink spreads across the surface, exceeding the theoretically defined area of the dot. This occurs due to several factors, including the viscosity of the ink, surface tension of the Inkjet inks, and the surface properties of the paper. For instance, inks with lower viscosity will spread more efficiently, increasing the likelihood of mechanical dot gain. On the other hand, uncoated papers, due to their porous nature, allow ink to be absorbed into the paper fibers, contributing to the printed dot's growth.

In addition to substrate properties, print resolution and dot shape variation influence mechanical dot gain. As print resolution increases, the printer's ability to reproduce individual dot elements accurately becomes limited. Distorted or irregular dots affect the overall quality of the printed image, leading to inconsistencies in tone and sharpness. This effect becomes more pronounced at higher resolutions, where even slight deviations in dot size can significantly impact image clarity.[14] Printers play a crucial role in maintaining high print quality. They must account for the mechanical growth of dots by adjusting ink volume, print speed, and other settings based on the type of paper and ink being used. Failing to do so can lead to images that are darker or less sharp than intended, as the increased dot size alters the tonal balance of the print.[15]

In conclusion, technical knowledge of physical dot gain is crucial in print reproduction, especially in high-resolution and Inkjet printing. Understanding of the interaction between inks, paper substrates, and the mechanical behavior of the print system is essential to achieving precise and high-quality printed images.

Optical dot gain

Optical dot gain is a critical factor in print quality, occurring when light scatters and diffuses within the paper substrate, making printed dots appear more significant than their intended size. This phenomenon is distinct from mechanical dot gain, which results from spreading ink on the paper surface. The extent of optical dot gain is influenced by the composition and structure of the paper, including its smoothness, opacity, and fiber content. For instance, paper substrates with higher mechanical pulp content tend to scatter light more, leading to a larger perceived dot size.[16]

Several prediction models for color or tone reproduction have been proposed based on macroscopic measurements. These include the Murray–Davies equation,[17] the Yule–Nielsen equation,[18] the Neugebauer model,[19] and the Yule–Nielsen modified Neugebauer model.[20] Other models include the Clapper–Yule model,[21] its extended versions,[22,23] the Williams–Clapper model,[24] and the extended Williams–Clapper model,[25] as well as a generalized model combining the Clapper–Yule and Williams–Clapper approaches.[26] Additionally, the Kubelka–Munk model[27] and its revised form[28] have been developed alongside the Saunderson model.[29] Some models also take into account factors such as ink penetration into paper[30] and the fluorescent effect.[31,32] The study of dot gain originally began with the simplest model for predicting print reflectance, the Murray-Davies equation. However, the more plausible description of the optical dot gain method based on the Monte Carlo approach was given in the works of Modrić *et al*.[33,34] and Itrić *et al*.,[35,36] where they developed an experimental method for accurately determining the optical component of dot gain by eliminating the mechanical dot gain. The research demonstrated that the Lorentzian function better describes the point spread function (PSF) in paper compared to the Gaussian function, which improves the optimization of optical and printing characteristics of paper. Additionally, by applying Monte Carlo simulations to model photon scattering in paper, precise separation of the optical and mechanical components of dot gain was achieved. The results showed that the Lorentzian function better describes the PSF in paper, significantly improving print quality and predicting paper behavior.

The challenge in studying optical dot gain is separating its effects from those of mechanical dot gain. Previous methods struggled to distinguish these two components accurately because total dot gain is a combination of optical and mechanical influences. The research highlighted in this text introduces a new approach by focusing

on the interaction of light with the substrate, eliminating the mechanical contribution. This allows for a clearer understanding of how optical dot gain impacts the overall print quality.

One of the critical tools for analyzing optical dot gain is the point spread function (PSF),[37] which describes how light spreads from a point source through a medium. The study revealed that optical dot gain is better modeled using a Lorentzian function than the traditional Gaussian function (contributions have different physical origins). The Lorentzian model more accurately reflects the broad scattering effect of light, particularly in papers with high mechanical pulp content, which tend to have more comprehensive PSF profiles and, therefore, greater optical dot gain.

This research underscores the importance of paper composition in controlling optical dot gain. Papers with rougher textures or higher fiber content scatter light more, leading to increased optical dot gain, while smoother papers exhibit less scattering. By accurately modeling optical dot gain using the Lorentzian function, researchers and manufacturers can better predict and control print outcomes, improving the clarity and sharpness of printed images.[38,39]

Optical dot gain typically accounts for about 30% of total dot gain, with mechanical dot gain contributing the remaining 60-70%, depending on the paper and printing method. While mechanical dot gain is influenced by ink viscosity and printing pressure, optical dot gain is governed primarily by the paper's ability to scatter light. Understanding the relative contributions of these components allows for better management of dot gain during the printing process, leading to higher print precision and consistency.

The findings of this study highlight the potential for using the Lorentzian model to simulate paper performance in a virtual environment. This enables manufacturers to test and optimize paper substrates before production, saving time and reducing costs. In conclusion, the study provides strong evidence that the Lorentzian function offers a more accurate description of optical dot gain than the Gaussian model, paving the way for improved printing technologies and paper development.

Overall dot gain

The total dot gain of the raster value is the sum of the physical (mechanical) and optical dot gain. Jackson (1990) defined the physical dot gain of the screen value as the total physical dot gain in the size of the print elements that occurs during each step of transferring the image to the printed paper. Classical printing can occur during the process of separating colors, making printing forms, and during the actual application (transfer) of ink from the printing form to the printing substrate. The digital inkjet technique is created only as a result of controlled spraying, *i.e.*, the capillary expansion of the ink droplets.[40]

To clarify the phenomenon and terminology related to the problem of the total increase in screening, a model of a printing system is applied in which the original is generated in a computer. The resulting increase is called dot gain. Figure 1 (a) shows the total dot gain of the smallest printing element (print dot).
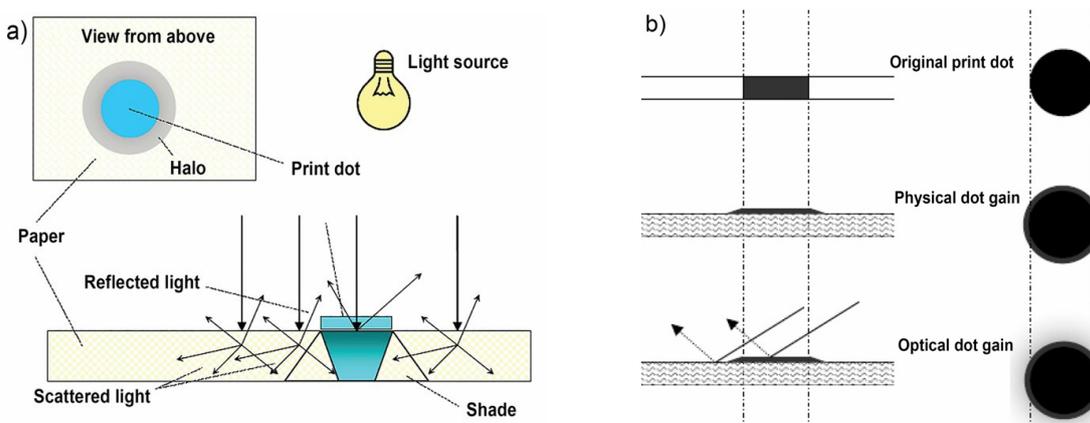

Figure 1: Phenomenon of creation of the total dot gain: a) Simplified illustration of creation of optical dot gain; b) Final reproduction of printing element

Inkjet printing of varnish for metalized foil adhesion

Inkjet printing technology for varnish application, combined with metalized foils, represents a cutting-edge method for achieving high-quality metalized effects on various printed materials. This process merges the precision of inkjet printing with the visual impact of metallic foils, making it a popular choice in the graphics industry, particularly for applications requiring a premium look, such as luxury packaging, high-end labels, promotional materials, and decorative printed designs. Unlike solid metal surfaces, which have distinct optical properties compared to paper and plastic substrates, screened metallic surfaces produce a unique optical dot gain, enhancing the overall visual experience by adding depth, shimmer, and reflectivity to printed designs.

Various decorative coating processes, including painting, powder coating, anodizing, electroplating, and an array of specialized printing and coating techniques, drive the increasing use of metalized surfaces in the graphics industry. These processes are employed across various industries, from automotive customization to architectural coatings, packaging, and glass and ceramic decoration. Among these, printing technologies stand out for their ability to create intricate and detailed metalized halftone designs, using small printed elements to achieve the desired effects.

Creating metalized halftones on standard paper substrates often involves the indirect cold-hot application of metalized foils. This method begins with precisely applying a UV-curable varnish using piezo Inkjet technology. The inkjet printer applies the varnish controlled, ensuring that the adhesive is placed exactly where the desired metalized effect is. This is followed by thermal lamination with the metalized foil, where heat is applied to bond the foil to the varnished areas. After the lamination, the foil is selectively peeled away, leaving a highly reflective, metallic finish only on the varnished sections. The result is a sharp, high-contrast design that mimics the appearance of metal, but with the flexibility and affordability of printing on standard substrates like paper or plastic.

A vital advantage of this method is its ability to produce exact and intricate metallic effects without the need for expensive traditional tools, such as engraved dies used in hot foil stamping. Inkjet varnish application allows for design flexibility, enabling the creation of custom patterns, gradients, and textures that would be difficult to achieve using conventional methods. Additionally, this process is ideal for short-run, customized projects, as it eliminates the setup costs associated with traditional metalized printing techniques.

Traditional reflective densitometers are ineffective in assessing the quality of metalized reproductions due to the complex reflective properties of these surfaces. Since metalized surfaces interact with light differently than standard printed surfaces, densitometers are ineffective in accurately assessing the quality of metalized reproductions. Instead, methods based on image analysis and evaluation of the total transferred surface are employed to measure the effectiveness of the metalized finish.[41] These methods allow for a more precise measurement of the metalized elements, ensuring that the desired coverage and reflective qualities are achieved consistently, making it ideal for high-end packaging, labels, and decorative printed materials.

Furthermore, the unique interaction between light and metalized surfaces results in a different optical dot gain than in traditional ink-based printing. This phenomenon occurs because the metallic surface reflects light, enhancing the visual contrast between the printed and non-printed areas, creating a more pronounced halftone effect. As a result, metalized halftones have a distinct aesthetic that is particularly well-suited for luxury packaging, where the goal is to catch the viewer's eye with a sophisticated, high-gloss finish.

In addition to its visual appeal, the combination of Inkjet printing with metalized foils offers several practical benefits. The ability to print directly onto substrates using UV-curable varnish means the process is more environmentally friendly than traditional solvent-based printing methods. UV curing allows for faster production times, as the varnish hardens instantly under UV light, reducing the need for lengthy curing processes. Moreover, using metalized foils adds a protective layer to the printed surface, enhancing the durability and scratch resistance of the final product.

Overall, Inkjet varnish printing with metalized foil transfer represents a significant advancement in printing technology, offering a flexible, precise, and cost-effective solution for creating stunning metalized effects. As the demand for high-quality,

visually striking packaging and printed materials continues to grow, this technology will likely play an increasingly important role in the graphics and printing industries, enabling brands to differentiate their products with eye-catching, reflective designs that stand out on the shelf.

EXPERIMENTAL

We used only the highest quality papers in the experiment, such as UPM Finesse silk semigloss double-coated cardboard (grammage 300 g/m^2).[42] The characteristics of this printing substrate are: high ISO brightness (100%), CIE whiteness (127.0) and opacity (99.8%). Due to the silk finishing, its smoothness PPS 10 is 25 μm, with a low gloss value (Hunter and Lehman Gloss 25%).

For print quality evaluation (gold halftone surface), we used four screen surfaces generated with dots print element perimeter: $d_1 = 0.10$ mm; $d_2 = 0.25$ mm; $d_3 = 0.50$ mm; $d_4 = 0.75$ mm. A high-quality print resolution of 1200 × 3600 dpi (electrophotographic reference) was used instead of a digital reference to achieve the most realistic conditions possible. Four dot surfaces were screened in the bitmapped image from PDF format using the Hikari KM IC602 processor. This black and white EP reference imprint contains a black Simitri powder toner applied to a Konica Minolta Accurio Print C3080 printing machine.[43]

The authors of this paper show a new method for testing the efficiency realization of gold halftones (around 50% TV surface coverage) created with four dot diameters. In the main experiment, we used identical mat fine art cardboard and gradually varied the amount of UV-LED cured inkjet varnish (applied in the machine and cross directions). To test dot gain, the effectiveness of this method in producing a metallic visual dot sample, we utilize three different thicknesses of UV-LED varnish (29 μm, 43 μm, and 58 μm) with the aid of inkjet heads KM1024 iLHE-30, with constant printing speeds of 0.30 m/s.

The final cold-hot samples were produced on a commercial Jetvarnish 3DS film varnishing and laminating machine.[44] The printing unit comprises five piezo Inkjet print heads type KM 1024 LHE-30.[45] It also contains two UV LED lamps emitting a wavelength of 395 nm. The first LED UV lamp has 4x5 W (four modules) power, while the second LED UV lamp has 12 W (one module). Using MGI UV Inkjet curing varnish, three different coating layers were printed (29 μm, 43 μm, and 58 μm). The Jetvarnish machine featured MGI JVTi 3.3.0.5 software. Data on the application of LED UV varnish were obtained indirectly (not through physical measurement), but from the manufacturer's data system. The glossy varnish JV3DS contains the next formulation: acrylic monomers and polymers, photoinitiators, and various additives. The main ingredient is the polymer diphenyl (2,4,6-trimethyl benzoyl) and phosphine oxide $(CH_3)_3C_6H_2COP(O)(C_6H_5)_2)$.[46]
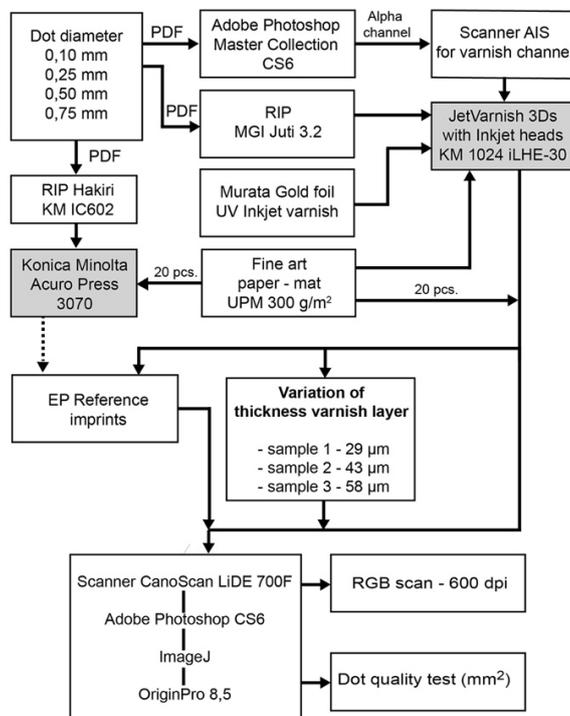

Figure 2: Chronological flow of the experiment

In experimental printing, Murata Gold-type foil was used to create the final gold halftone surface. After the varnishing and UV curing, a metalized foil application unit was used. The temperature transfer

was controlled in 6 zones. In our case, a constant heater temperature of 105 °C was used. The foil application was controlled with an AIS scanner (180 defined check positions) to achieve the exact position of the dots image. The varnish channel was created using the TIFF alpha channel generated by Adobe Photoshop CS6 25.7.[47]

Three different samples were printed, and the thickness of the varnish varied before contact with the metalized foil (29 μm, 43 μm, and 58 μm). After that, for gold halftone image analysis, all samples were digitalized using a CanoScan LiDE 700F scanner (resolution of 600 dpi, RGB image in TIFF format). Before image analysis, all dot sample images were cropped in Adobe Photoshop in grayscale format 9×6 cm with the resolution of 600 dpi). The final analysis and results were obtained using the open-source program ImageJ version 1.5.3, with a designed macro program to calculate dot surface coverage. Using the detected black pixels, the total area of print elements was calculated. For this location, we used the program OriginPro version 8.5. Figure 2 shows the flow chart of the experiment.

RESULTS AND DISCUSSION

Printed products, which often contain halftone images as information, have small print elements of different geometric shapes. In standard printing procedures, a circular shape is primarily used. However, for this research, we have taken a more meticulous approach. We analyzed four dot surfaces with dimensions of 5 x 5 cm, each generated with print elements (dots) of varying diameters: $d_1 = 0.100$ mm, $d_2 = 0.250$ mm, $d_3 = 0.500$ mm, and $d_4 = 0.750$ mm. The surface coverage of all samples was 25% TV. We conducted three experimental series of gold-gridded samples, each treated with UV LED drying varnish of different thicknesses: 29 μm, 43 μm, and 58 μm. The results, presented in Figures 3, 4, 5, and 6, showcase the digitized samples of the four experimental dot surfaces printed on a Konica Minolta AccurioPrint C3080 machine (reference) and a Jetvarnish 3DS foil printing machine.

The surface of the realized reference samples ((b1) in Figs. 3-6) with the minor dot elements of diameter $d_1 = 0.100$ mm (printed with ROS EP technology = Raster Optical Scanner ElectroPhotography) has a regular geometric structure and a total surface area of $A_{ref} = 34.318$ mm². The gold print of this sample, which was realized by applying UV varnish with a thickness of 29 μm ((b2) in Figs. 3-6), does not retain the regular structure of round print dots and achieves the minor surface for $\Delta A_{Ref\_S1} = -26.711$ mm². Applying the UV varnish setting to 43 μm ((b3_Sample 2) in Figs. 3-6) results in more intense varnishing of 0.100 mm dot elements that connect, forming a uniform surface coverage of $A_{S2} = 48.272$ mm². Such a surface is not homogeneous and contains many white cracks. Compared to the reference, this increase amounts to $\Delta A_{Ref\_S2} = 13.945$ mm². Thus, the area compared to the reference ((b4) in Figs. 3-6) will increase significantly ($\Delta A_{Ref\_S3} = 81.501$ mm²). An initial rise in the varnish coating of 14 μm will achieve a deviation of the printed surface by $\Delta A_{S1\_S2} = 40.666$ mm², while a further increase in the coating of 15 μm will achieve an increase in the surface of $\Delta A_{S2\_S3} = 67.558$ mm².
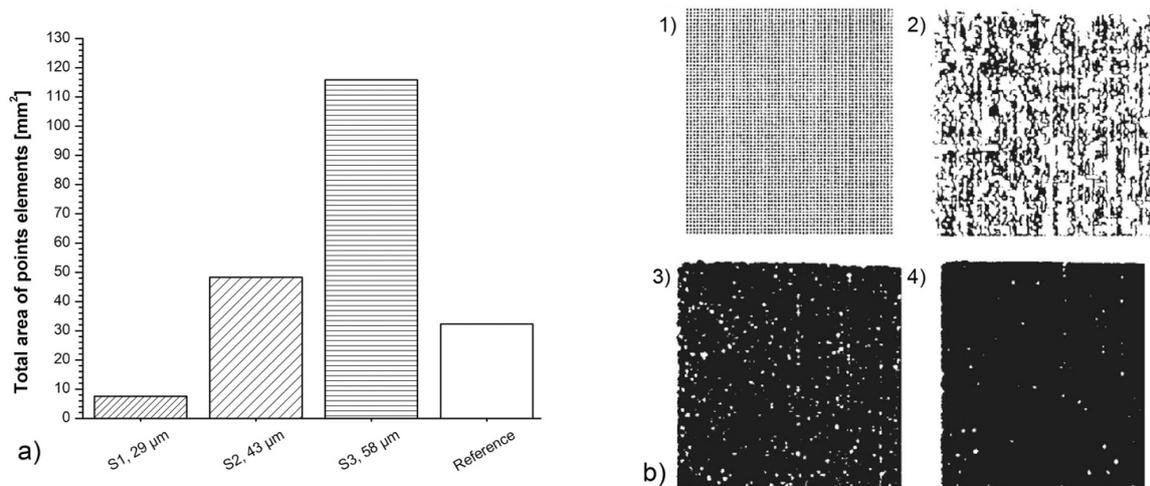

Figure 3: Reproductions of gold perimeter dots of 0.100 mm: a) total area of EP reference and samples with three different UV varnish layers; b) bitmap image of samples after gold foil lamination (1 = reference; 2 = layer of 29 μm; 3 = layer of 43 μm; 4 = layer of 59 μm)
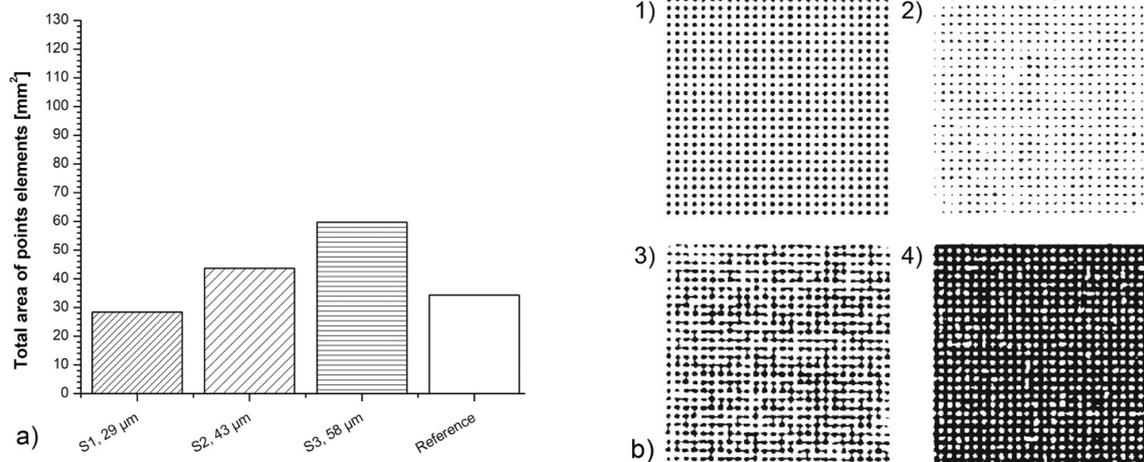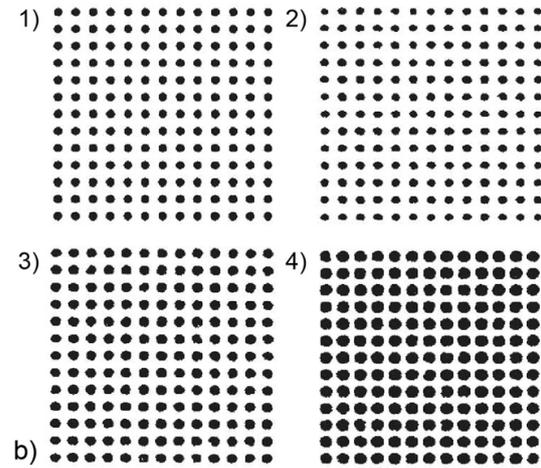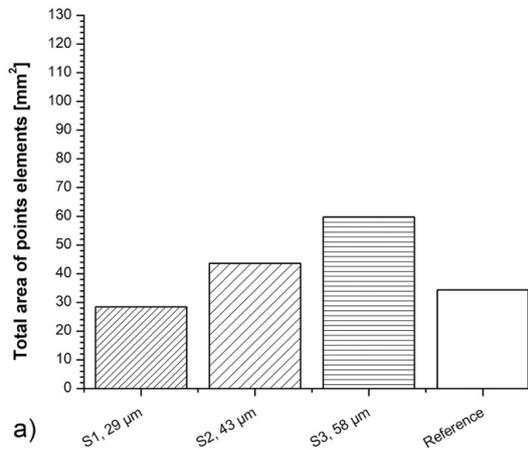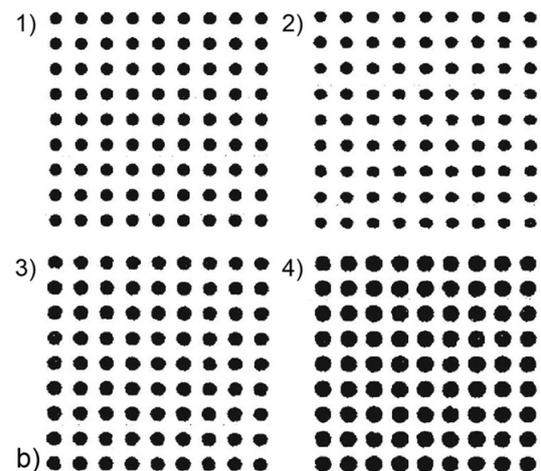
Figure 4: Reproductions of gold perimeter dots of 0.250 mm: a) total area of EP reference and samples with three different UV varnish layers; b) bitmap image of samples after gold foil lamination (1 = reference; 2 = layer of 29 μm; 3 = layer of 43 μm; 4 = layer of 59 μm)

Thus, the size of the elements of 0.100 mm will reach the most significant deviations.

The surface of the realized reference samples with dot elements of diameter $d_2 = 0.250$ mm ((b1) printed with ROS EP technology, in Figs. 3-6) has a very regular geometric structure and a total surface area of $A_{ref} = 34.330$ mm^2. The gold print with a surface coverage of 25% TV (realized by a cold-hot lamination process with a pre-applied UV varnish of 29 μm) retains the regular grid structure and achieves a smaller surface by $\Delta A_{Ref\_S1} = -5.8995$ mm^2 (Fig. b2). Increasing the application of UV varnish by 14 μm ((b3_Sample 2) in Figs. 3-6), in some places, leads to the connection of elements with a diameter of 0.250 mm, which results in a light closing of the surface ($\Delta A_{Ref\_S2} = 9.325$ mm^2). The maximum application of UV varnish (Fig. b4_Sample 3) will completely cover the 5 x 5 cm gridded surface (a whole tone is created). In doing so, the area will increase compared to the reference ($\Delta A_{Ref\_S3} = 25.455$ mm^2). Thus, an experimental increase in the varnish coating of 14 μm will result in an increase in the surface by $\Delta A_{S1\_S2} = 14.5495$ mm^2, while a further increase in the coating of 15 μm will increase the surface ($\Delta A_{S2\_S3} = 16.100$ mm^2).

The surface of the realized reference samples with dot elements with a diameter of $d_3 = 0.500$ mm ((b1) in Figs. 3-6) is reproduced in the best quality (compared to the printed EP reference, they have a regular geometric structure, where the total area of the reference is $A_{ref} = 34.327$ mm^2. The gold print of the surface with a previously applied UV varnish of 29 μm ((b2) in Figs. 3-6) has a regular grid screen structure and achieves a minor surface deviation for $\Delta A_{Ref\_S1} = -5.831$ mm^2. Setting the UV varnish to 43 μm ((b3_Sample 2) in Figs. 3-6) will maintain a stable gold print with a slightly noticeable increase in the analyzed surface compared to the reference ($\Delta A_{Ref\_S2} = 9.393$ mm^2). The most significant experimental application of UV varnish (58 μm) will significantly increase the 5 x 5 cm screened area in which the round print dots remain open ((b4) in Figs. 3-6). In comparison, the surface will increase compared to the reference ($\Delta A_{Ref\_S3} = 25.494$ mm^2). By experimentally increasing the varnish coating of 14 μm, a uniform increase of the gold surface was achieved ($\Delta A_{S1\_S2} = 15.224$ mm^2; $\Delta A_{S2\_S3} = 16.101$ mm^2).

The surface of the realized reference samples with dots elements of diameter $d_4 = 0.750$ mm retains the correct reproduced structure. The printed EP reference has the exact round geometric shape of the surface $A_{ref} = 34.339$ mm^2. The gold print of the surface with a previously applied UV varnish of 29 μm retains the regular grid structure of the screen and realizes a slightly smaller surface deviation for $\Delta A_{Ref\_S1} = -11.505$ mm^2. Related to the reference, the application of UV varnish of 43 μm (Sample 2) will maintain a stable gold print with a slightly higher increase in the analyzed area ($\Delta A_{Ref\_S2} = 10.193$ mm^2). However, the most extensive application of UV varnish (Sample 3) will significantly increase the screened surface. The round print dots become

more comprehensive and remain open. In doing so, the area will increase compared to the reference ($\Delta A_{Ref\_S3} = 31.785$ mm^2). With an experimental increase in the varnishing of 14 µm,

the trend of a uniform increase in the achieved gold surface remains ($\Delta A_{S1\_S2} = 21.695$ mm^2; $\Delta A_{S2\_S3} = 21.590$ mm^2).
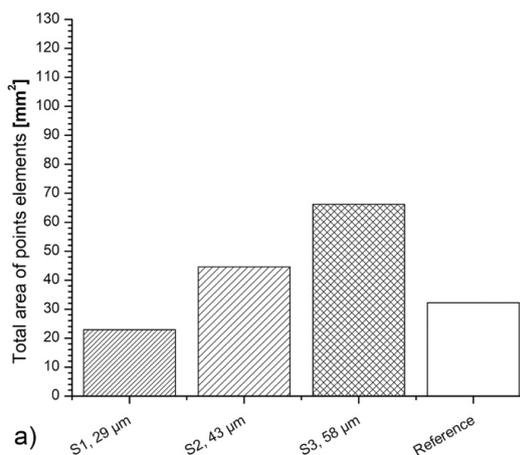

Figure 5: Reproductions of gold perimeter dots of 0.500 mm: a) total area of EP reference and samples with three different UV varnish layers; b) bitmap image of samples after gold foil lamination (1 = reference; 2 = layer of 29 µm; 3 = layer of 43 µm; 4 = layer of 59 µm)

Figure 6: Reproductions of gold perimeter dots of 0.750 mm: a) total area of EP reference and samples with three different UV varnish layers; b) bitmap image of samples after gold foil lamination (1 = reference; 2 = layer of 29 µm; 3 = layer of 43 µm; 4 = layer of 59 µm)

CONCLUSION

Related to the reference surface (25% TV), all experimental samples with the smallest amount of UV varnish application (29 µm) achieve a smaller printed surface. A more significant amount of adhesive varnish creates more prominent printed elements with a regular geometric structure and regular dot diameters.

With a low varnish dose, the smallest tested printing elements with a diameter of 0.100 mm are entirely unrecognizable. Such surface is stained, and the total gold printed surface is

reduced by 22%. A more significant amount of adhesive varnish achieves the connection of printing elements with the loss of geometric structure and visible diameters to be realized (the surface of Sample 2 increased by 140% and that of Sample 3 – by 337%). Therefore, the KM1024 iLHE-30 Inkjet head is unsuitable for printing circular elements with a diameter smaller than 0.100 mm.

Round printing elements with a diameter of 0.250 mm will achieve significant surface deviations by experimental printing. Samples with

the lowest UV varnish application (29 μm) will have a smaller surface than EP references. The diameters of such dots give a barely visible golden grid pattern (area reduced by 17.2%). A more significant amount of lacquer achieves geometrically properly realized diameters whose edges meet (the surface area of Sample 2 increased by 27.4% and that of Sample 3 – by 74.4%).

Round printing elements with a diameter of 0.500 mm will be reproduced in the best quality with the Inkjet head KM1024 and LHE-30. Samples produced with a coating of 29 μm will achieve a slightly smaller surface compared to EP references (surface reduced by 17%). At the same time, a more significant amount of varnish will achieve geometrically properly realized diameters (the surface of Sample 2 increased by 27.2% and that of Sample 3 – by 74.1%).

Round printing elements with a diameter of 0.750 mm retain the quality of reproduced gold elements. Samples made with a varnish deposit of 29 μm will remain somewhat smaller in area than the reference. However, a more significant amount of applied varnish will achieve geometrically regular point diameters, the surface of which is additionally increased (Sample 2 = 29.6% and Sample 3 = 92.4%).

To achieve better results, it will be necessary to use an Inkjet head with a smaller print nozzle that will achieve a smaller volume of UV varnish droplets (elements smaller than 0.250 mm). To achieve the optimal pattern, it is necessary to ensure the use of correct input files, in which the dimensions of the realized printing elements can be corrected. Therefore, further research will be directed toward testing new printing substrates, other types of piezo Inkjet heads, and modification of input files.

REFERENCES

1   G. G. Field, "Color and Its Reproduction", GATF Press, 2nd ed., Pittsburg, 1999
2   A. Leutert, "Allgemeine Fachkunde der Drucktechnik", Baden-Verlag, 11th ed., 1993
3   G. Goldmann, "The World of Printers, Oce Printing Systems GmbH", Dusseldorf, 2004, pp. 204-208
4   H. Kipphan, "Handbook of Print Media Technologies and Production Methods", Springer-Verlag, Berlin Heidelberg, 2001, pp. 100-104
5   A. Kraushaar, "Process Standard Offset (PSO) and Process Standard Digital (PSD) – Printing the Expected in Offsetand Digital Printing", Munich, 2022, pp. 1–25
6   A. Schuster, *Astrophys. J.*, **21**, 1 (1905), (Reprinted in D. H. Menzel, "Selected Papers on the Transfer of Radiation", Dover, New York, 1966)
7   P. Kubelka and F. Munk, *Z. Techn. Phys.*, **12**, 593 (1931)
8   P. Kubelka, *J. Opt. Soc. Am.*, **38**, 448 (1948), https://doi.org/10.1364/JOSA.38.000448
9   J. Saunderson, *J. Opt. Soc. Am.*, **32**, 727 (1942), https://doi.org/10.1364/JOSA.32.000727
10   P. Emmel and R. D. Hersch, *IEEE Computer Graphics and Applications*, **19**, 54 (1999), https://doi.org/10.1109/38.773964
11   P. Emmel, "Modèles de prédiction couleur appliqués et l'impression jet d'encre", These No 1857, École Polytechnique Fédérale de Lausanne, 1998, pp.71-101
12   S. Mourad, P. Emmel, K. Simon and R. D. Hersch, in *Procs. IS&T 10th Color and Imaging Conference*, 2002, pp. 298-304, https://doi.org/10.2352/CIC.2002.10.1.art00056
13   I. Heikkilä and S. Karttunen, in *Procs. IARIGAI 25th Research Conference*, Pittsburgh, 1998, pp. 1–22
14   J. A. C. Yule and W. J. Nielsen, *Proc. Tech. Assoc. Graphic*, **3**, 65 (1951)
15   F. R. Clapper and J. A. C. Yule, *J. Opt. Soc. Am.*, **43**, 600 (1953), https://doi.org/10.1364/JOSA.43.000600
16   J. S. Arney, *J. Imaging Sci. Technol.*, **41**, 633 (1997), https://doi.org/10.2352/J.ImagingSci.Technol.1997.41.6.art00013
17   A. Murray, *J. Franklin Inst.*, **221**, 721 (1936), https://doi.org/10.1016/S0016-0032(36)90524-0
18   R. D. Hersch, P. Emmel, F. Collaud and F. Crete, *J. Electron. Imaging*, **14**, 033001 (2005), https://doi.org/10.1117/1.1989987
19   J. A. S. Viggiano, in *Procs. TAGA*, 1990, pp. 44–62
20   P. Emmel and R. D. Hersch, *J. Imaging Sci. Technol.*, **44**, 351 (2000)
21   G. Rogers, *Color Res. Appl.*, **25**, 402 (2000), https://doi.org/10.1002/1520-6378(200012)25:6<402::AID-COL4>3.0.CO;2-6
22   F. C. Williams and F. R. Clapper, *J. Opt. Soc. Am.*, **43**, 595 (1953), https://opg.optica.org/josa/abstract.cfm?URI=josa-43-7-595
23   J. D. Shore and J. P. Spoonhower, *J. Imaging Sci. Technol.*, **45**, 484 (2001)
24   M. Hebert and R. D. Hersch, *J. Imaging Sci. Technol.*, **48**, 363 (2004)
25   L. Yang and B. Kruse, *J. Opt. Soc. Am. A*, **21**, 1933 (2004), https://doi.org/10.1364/josaa.21.001933
26   J. L. Saunderson, *J. Opt. Soc. Am.*, **32**, 727 (1942), http://www.opticsinfobase.org/josa/abstract.cfm?URI=josa-32-12-727
27   L. Yang and B. Kruse, in *Procs. NIP & Digital Fabrication Conference* **17**, 731 (2001), https://doi.org/10.2352/ISSN.2169-4451.2001.17.1.art00065_2

28   P. Emmel and R. D. Hersch, in *Proc. 5th IST/SID Color Imaging Conference*, Santa Ana, 1997, pp. 70-77

29   R. D. Hersch, *Appl. Opt.*, **47**, 6710 (2008), https://doi.org/10.1364/AO.47.006710

30   D. Modrić, S. Bolanča and R. Beuc, *J. Imaging Sci. Technol.*, **53**, 020201 (2009), https://doi.org/10.2352/J.ImagingSci.Technol.2009.53.2.020201

31   D. Modrić, K. Petric Maretić and A. Hladnik, *Appl. Opt.*, **53**, 7854 (2014), http://dx.doi.org/10.1364/AO.53.007854

32   K. Itrić, D. Modrić and M. Milković, *Nord. Pulp Pap. Res. J.*, **33**, 542 (2018), https://doi.org/10.1515/npprj-2018-3054

33   K. Itrić, D. Modrić, M. Milković and A. Divjak, *Nord. Pulp Pap. Res. J.*, **34**, 534 (2019), https://doi.org/10.1515/npprj-2019-0008

34   A. C. Hubler, in *Proc. IS&T's NIP13 Conference*, 1997, pp. 481-484

35   C. L. Killeen, *GATF World*, **7**, 27 (1995)

36   S. Gustavson, Doctorate Thesis, No 492, Linköping Studies in Science and Technology, Linköp, 1997

37   L. L. Jackson, *GATF World*, **2**, 1 (1990)

38   I. Majnarić, M. Modrić, D Valdec and K. Milković, *Coatings*, **14**, 604 (2024), https://doi.org/10.3390/coatings14050604

39   UPM Finesse silk, Retrieved from (2022, September 21), https://www.upmpaper.com/products/papercatalogue/categories/sheet-fed-offset-papers/upm-finesse-silk/

40   Konica Minolta AccurioPress C3080, Retrieved from (2024, June 22), https://www.konicaminolta.eu/en/businesssolutions/products/production-printing/colour/accuriopress-c30703080/introduction.html

41   Konica Minolta MGI Jetvarnish 3DS, Retrieved from (2022, May 21), https://www.konicaminolta.eu/getmedia/31987dc8-d933-40a3-b988-fd53c0421f6e/MGI-JETVarnish-3DS-iFoil-S-Datasheet.pdf.aspx

42   Konica Minolta Inkjet Printhead Lineup Catalogs, Retrieved from (2024, June 22), https://www.konicaminolta.com/globalen/inkjethead/products/inkjethead/pdf/ij_lineup_jpn_eng.pdf.

43   Konica Minolta Material Safety Data Sheet for JV3DS - LED Varnish, Retrieved from (2023, May 12), https://www.konicaminolta.jp/about/csr/environment/communication/msds/pdf/mgi/MGI_SDS-MSDS_n°58-JV3DS-LED_VARNISH_PN_10143S_020522.pdf

44   Konica Minolta AIS SmartScaner, Retrieved from: (2024, June 22), https://www.printingnews.com/softwareworkflow/product/12252965/mgi-digital-graphic-technology-ais-smartscanner